

Effect of an electric field on dewetting transition of nitrogen-water system

Qi Feng(冯琦), Jiaxian Li(厉嘉贤), Xiaoyan Zhou(周晓艳), and Hangjun Lu(陆杭军)

Citation: Chin. Phys. B, 2022, 31 (**3**): 036801. DOI: 10.1088/1674-1056/ac1e21
Journal homepage: http://cpb.iphy.ac.cn; http://iopscience.iop.org/cpb

What follows is a list of articles you may be interested in

Dielectrowetting actuation of droplet: Theory and experimental validation

Yayan Huang(黄亚俨), Rui Zhao(赵瑞), Zhongcheng Liang(梁忠诚), Yue Zhang(张月), Meimei Kong(孔梅梅), and Tao Chen(陈陶)

Chin. Phys. B, 2021, 30 (**10**): 106801. DOI: 10.1088/1674-1056/ac1926

Strain-tunable electronic and optical properties of h-BN/BC_3 heterostructure with enhanced electron mobility

Zhao-Yong Jiao(焦照勇), Yi-Ran Wang(王怡然), Yong-Liang Guo(郭永亮), and Shu-Hong Ma(马淑红)

Chin. Phys. B, 2021, 30 (**7**): 076801. DOI: 10.1088/1674-1056/abe29d

Microdroplet targeting induced by substrate curvature

Hongguang Zhang(张红光), Zhenjiang Guo(郭振江), Shan Chen(陈珊), Bo Zhang(张博), Xianren Zhang(张现仁)

Chin. Phys. B, 2018, 27 (**9**): 096801. DOI: 10.1088/1674-1056/27/9/096801

Structure and dynamics of ordered water in a thick nanofilm on ionic surfaces

Ren Xiu-Ping, Zhou Bo, Li Lan-Ting, Wang Chun-Lei

Chin. Phys. B, 2013, 22 (**1**): 016801. DOI: 10.1088/1674-1056/22/1/016801

Effect of an electric field on dewetting transition of nitrogen-water system

Qi Feng(冯琦), Jiaxian Li(厉嘉贤), Xiaoyan Zhou(周晓艳)[†], and Hangjun Lu(陆杭军)[‡]

Department of Physics, Zhejiang Normal University, Jinhua 321004, *China*

(Received 10 July 2021; revised manuscript received 7 August 2021; accepted manuscript online 17 August 2021)

We investigate the influence of an external electric field on the dewetting behavior of nitrogen-water systems between two hydrophobic plates using molecular dynamics simulations. It is found that the critical distance of dewetting increases obviously with the electric field strength, indicating that the effective range of hydrophobic attraction is extended. The mechanism behind this interesting phenomenon is related to the rearrangement of hydrogen bond networks between water molecules induced by the external electric field. Changes in the hydrogen bond networks and in the dipole orientation of the water molecules result in the redistribution of the neutral nitrogen molecules, especially in the region close to the hydrophobic plates. Our findings may be helpful for understanding the effects of the electric field on the long-range hydrophobic interactions.

Keywords: dewetting transition, hydrophobic interactions, electric field

PACS: 64.70.F–, 68.03.Hj, 68.03.–g, 68.18.Jk **DOI:** 10.1088/1674-1056/ac1e21

1. Introduction

Hydrophobic interactions between nonpolar groups in water are important in many chemical processes and biological activities.[1–5] For example, it has been recognized that hydrophobic interaction as the major driving force plays a key role in folding of proteins and self-assembly of biomolecules in cells.[1,6–9] A fascinating effect appreciated recently is that, when two nanoscale hydrophobic objects approach each other and reach a critical separation, though large enough to accommodate water molecules, a dewetting (drying) transition will occur in the inter-object region. This behavior will lead to long-range hydrophobic attraction, resulting in hydrophobic collapse,[7,10] which is possibly relevant to collapse of multi-domain proteins and folding of heterogeneous globular proteins.[6,11] Although a great deal of work has concentrated on the hydrophobic effect in proteins,[12–15] a detailed understanding of its role as a driving force in protein folding and assembly still remains elusive. This is mainly due to the complex combination of hydrophobic and hydrophilic (charged residues) regions in proteins. Patel *et al.* have investigated how proteins coordinates do the functions of hydrophobic and hydrophilic regions to facilitate their biological functions.[16] They found that hydrophobic atoms on the protein surface situate their hydration waters at the edge of a dewetting transition, which can be triggered by an unfavorable perturbation. The hydration shells of diverse proteins undergo collective dewetting, which is originated from the collective motion of water hydrogen bond networks surrounding hydrophobic surfaces. Moreover, the breathing gases are also dissolved in the physiological solutions. Recently, the existence of aggregated gas molecules at the water-solid interface was confirmed.[17–22] In our previous study, we found that the nitrogen molecules prefer to aggregate in the vicinity of the two hydrophobic surfaces and exclude water molecules. The effective range of hydrophobic attraction between the two nanoscale plates is enhanced by the aggregated nitrogen molecules.[23] This aggregation behavior is proposed to be related to the gas toxicity.[24] It has been recognized that existence of charged residues in proteins greatly reduces hydrophobicity. How an electric field created by charged residues affects hydrophobicity of hydrophobic regions in proteins and aggregation behavior of gas in the solutions has remained challenge.

Considering the complicated structure of proteins and their complex surroundings, it is difficult to directly probe the hydrophobic effect in these complicated systems. It has been well recognized that idealized plates can usually be used as a model system to exploit some of the primary characteristics of hydrophobic interactions in complex biological systems.[25–29] In 1995, Wallqvist *et al.* observed a spontaneous dewetting transition between two large parallel hydrophobic plates by constant-pressure molecular dynamics simulations.[30] Weeks and coworkers provided a Lum–Chandler–Weeks (LCW) theory to explain the mechanism of hydrophobicity. The theory includes a component sustains interfaces, liquid–vapor phase equilibria and drying.[12] Using a combination of analytical theories and the coarse-grained model in simulations, researachers have studied water dewetting phenomena extensively.[10,31–33]

In this paper, we choose two nanoscale parallel hydrophobic plates to investigate effects of the external electric field on

[†]Corresponding author. E-mail: zxylu@zjnu.cn
[‡]Corresponding author. E-mail: zjlhjun@zjnu.cn

© 2022 Chinese Physical Society and IOP Publishing Ltd

the long-range hydrophobic interaction. The dewetting transition is found to be very sensitive to the external electric field. In our previous paper, we found that the nitrogen molecules trapped in water cages can be released by the external electric field.[34] Differently, here we find that the neutral nitrogen molecules are encapsulated in the nanoscale cavity between two hydrophobic plates when a uniform electric field is introduced. Correspondingly, the water molecules are driven out. The detailed mechanism is also discussed.

2. Methodology

The simulation framework is illustrated in Fig. 1. Two parallel hydrophobic plates with an area of 3.4 nm $\times$2.9 nm along the x–y plane separated by a distance were solvated in bulk water. The plates consist of a hexagonal arrangement of monolayer atoms with a bond length of 0.142 nm. Initially, 15 nitrogen molecules were randomly inserted in the space between the two hydrophobic plates. In order to investigate the effect of electric field on dewetting behavior, an electric field is applied along the z axis. In all simulations, the two plates were held and fixed with a specified separation from 1.3 nm to 2.9 nm.

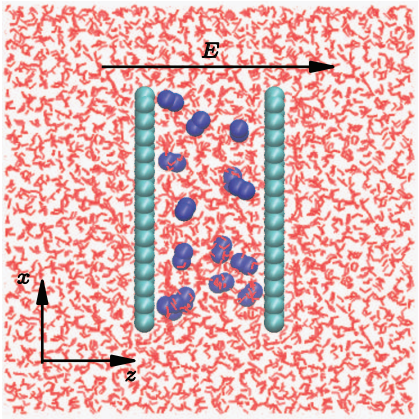


Fig. 1. Side view of the simulation framework generated using VMD. Cyan spheres and blue spheres represent atoms of model solid plates and atoms of nitrogen molecules, respectively. Water molecules are indicated by red lines. The simulation box is subjected to an electric field along the z axis. Here $0 \leq E \leq 0.8$ V/nm.

All the molecular dynamics simulations were performed by using the GROMACS simulation package 2016.5 in the NPT ensemble. A pressure of 1.0 bar is applied and a temperature of 300 K was maintained by using Berendsen thermostat.[35] The system contains 7513 water molecules. The SPC/E water model was employed.[36] The atoms of model solid plates were represented with Lennard–Jones (LJ) parameters: $\sigma_{ss} = 3.478$ Å and $\varepsilon_{ss} = 0.2267$ kJ/mol. The hydrophobic property of solid plates is determined by the LJ interactions between neutral solid plates and water molecules. The water-plate interactions were treated by an LJ potential with the parameters: $\sigma_{ws} = 3.3178$ Å, $\varepsilon_{ws} = 0.3838$ kJ/mol. The nitrogen atoms were modeled as uncharged LJ particles with the parameters of $\sigma_{NN} = 3.260$ Å, $\varepsilon_{NN} = 0.2888$ kJ/mol. The N–N interatomic distance is 0.14 nm, maintained by harmonic potentials with a spring constant of 1.280×10^6 kJ/mol·nm^2. We used the same parameters given in previous studies.[24,37] Periodic boundary conditions were applied in all directions. The long-range electrostatics interactions were handled by using the particle mesh Ewald (PME) method with a cutoff for real space of 1.4 nm.[38] The short-range van der Waals forces had a cutoff distance of 1.5 nm.

We performed a series of MD simulations with the plates fixed at various separations, with the magnitude of the electric field in the range of 0 to 0.8 V/nm. Under a given electric field, simulation time at each state point was 4 ns after the system had been equilibrated for 2 ns. A time step of 1 fs was used for all simulations.

3. Results and discussion

In order to explore the effect of electric field on the dewetting phenomenon, we have simulated the behavior of water between two nanoscale hydrophobic plates under various electric fields perpendicular to the plates. We calculated the average number of interplate water molecules for various separations between two parallel plates, which is usually chosen as the order parameter to analyze the phase behavior.

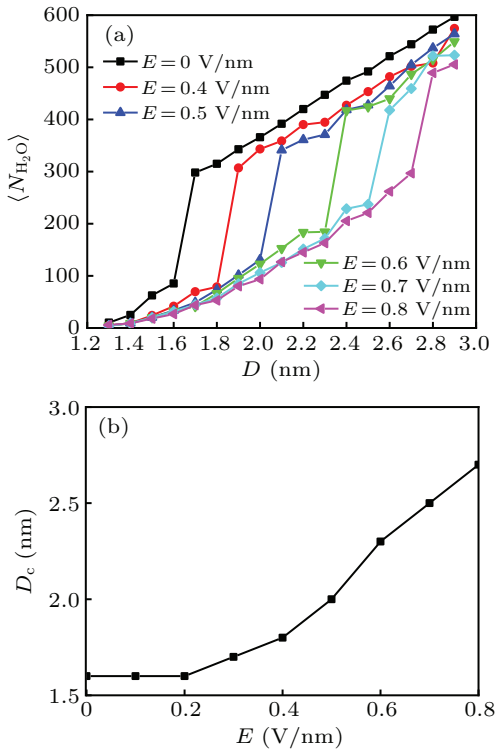


Fig. 2. Dewetting transitions: (a) average number of interplate water molecules as a function of the interplate distance for different electric fields, (b) critical distance D_c for the dewetting transition as a function of the electric field.

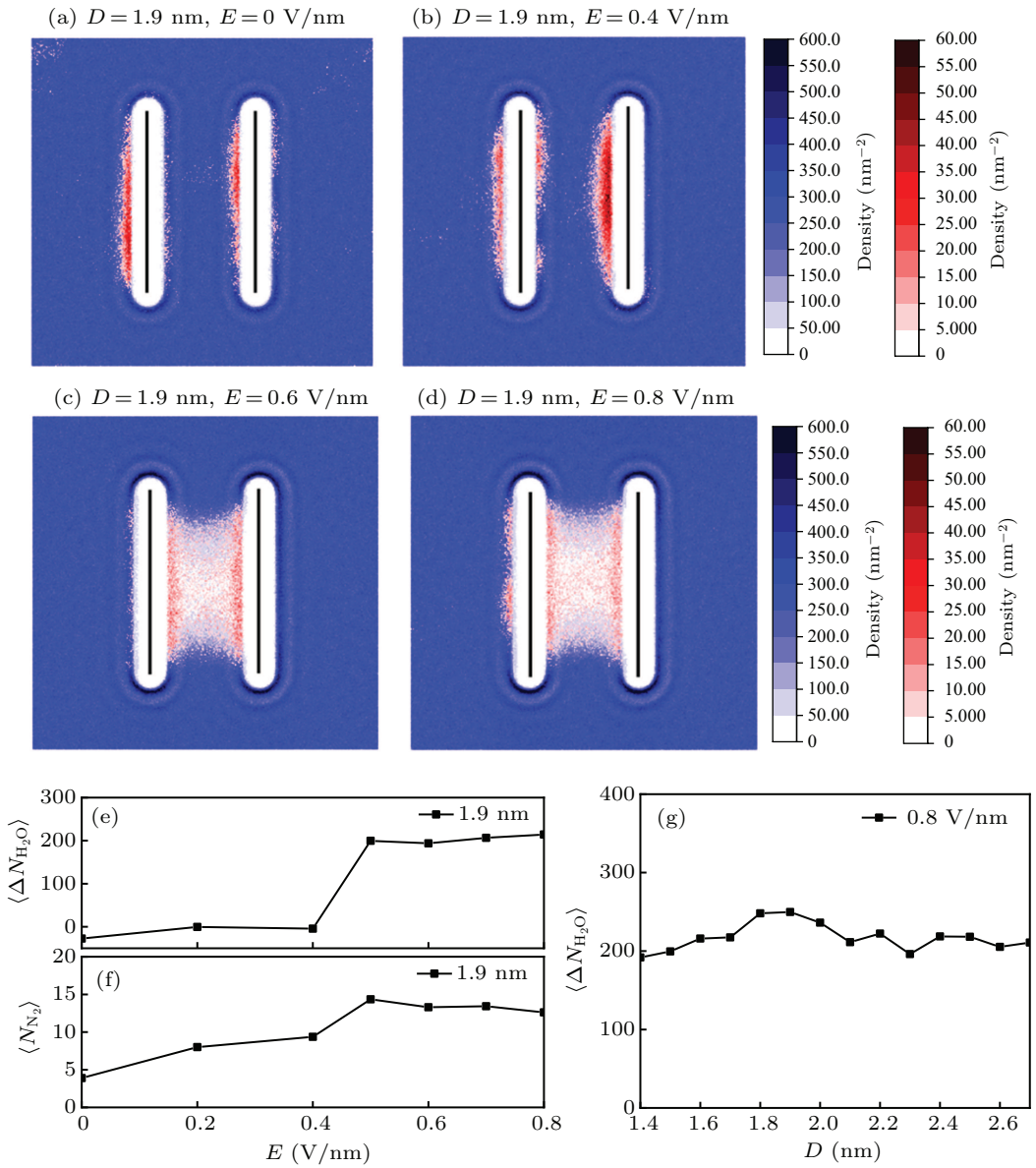


Fig. 3. (a)–(d) Probability density distributions of the water (blue) and nitrogen molecules (red) under different electric fields for plate separation $D = 1.9$ nm. (e) The difference between the number of interplate water molecules at the beginning and at the end of the simulation. (f) The number of nitrogen molecules in the interplate region as a function of electric field. (g) The change of the number of interplate water molecules before and after dewetting for systems with different plate separations.

The results are shown in Fig. 2(a). Here, the average is taken over the last 100 ps simulation data. In all cases, as the distance between two hydrophobic plates decreases from 2.9 nm to 1.3 nm, the average number of interplate water molecules first gradually decreases and then drops abruptly at a critical separation. This marked discontinuous behavior signifies a wetting/dewetting transition, analogous to a first-order phase transition. The distance between two plates at which the dewetting transition takes place is denoted by D_c. The value of D_c as a function of electric field is plotted in Fig. 2(b). It is obvious that the critical distance D_c of dewetting transition increases with the external electric field, indicating that, effectively, the external electric field can enhance the long-range hydrophobic interaction.

The distribution of nitrogen molecules between two plates plays a key role in dewetting transition. To investigate the influence of electric fields on the distribution of N_2 molecules, we calculated 2D probability density distribution of the water and nitrogen molecules averaged over the last 100 ps (Figs. 3(a)–3(d)). We also counted the number of nitrogen molecules confined in the interplate region, as shown in Fig. 3(f). The changes in the number of interplate water molecules at the beginning and at the end of the simulation are plotted in Fig. 3(e). Here the separation between the two plates, D, is 1.9 nm in these simulations. In the field-free case, as shown in Fig. 3(a), the system is in the water-filled state. Nitrogen molecules are adsorbed onto both sides of the plates and form molecular layers in the vicinity of the hydrophobic surfaces. Some nitrogen molecules escaped out to the bulk water and dissolved in the solvent. It is consistent with the

phenomena observed in previous studies.[39] When an electric field $E = 0.4$ V/nm is applied, the nitrogen molecules further accumulate at the surfaces of the plates (see Fig. 3(b)). The number of nitrogen molecules inside the interplate region increases from 4 to 9 (see Fig. 3(f)). Further increasing E will lead to a sudden dewetting transition (see Fig. 3(c)). The interplate water is expelled out and a cavity filled with nitrogen molecules forms. Correspondingly, the average number of nitrogen molecules inside the interplate region increases to about 14 (see Fig. 3(f)). From Figs. 3(c) and 3(d), we can see that the density of N_2 molecules in the interplate region is non-uniform. The probability of N_2 molecules staying in the vicinity of the inner surfaces of hydrophobic plates is higher than the other regions due to the van der Waals interaction between N_2 molecules and the plates. N_2 molecules in the center region are in the gas state, with low probability density. It should be noted that the total N_2 molecules in the system is 15. Therefore, when the electric field is further increased after dewetting, the number of nitrogen molecules and the water molecules inside the interplate remain approximately the same (see Figs. 3(e) and 3(f)). It is obvious that once the nanocavity forms, its volume will remain unchanged under the different electric fields.

We also examine the volume of the cavities formed in other systems with different plates seperations. The volume of the cavity is measured by counting the number of water molecules expelled from the two plates. The result is shown in Fig. 3(g). At $E = 0.8$ V/nm, for all configurations with different separations, the dewetting transitions will take place. The number of water molecules expelled from the inter-plate region due to the dewetting is denoted by ΔN_{H_2O}, the average value $\langle \Delta N_{H_2O} \rangle$ for different D under the same external electric field is about 210. Our simulation results show that the fluctuation of ΔN_{H_2O} is about 10% arising from thermal fluctuations. Thus, within error estimates, ΔN_{H_2O} keeps almost unchanged for different interplate distances under the same electric field. It is indicated that the volume of the nanocavity is independent of the interplate separations. From the above analysis, it can be seen that the electric field helps nitrogen molecules enter the interplate region and accumulate on the surfaces of the plates. The aggregation behavior of N_2 is conducive to the dewetting transition.[23]

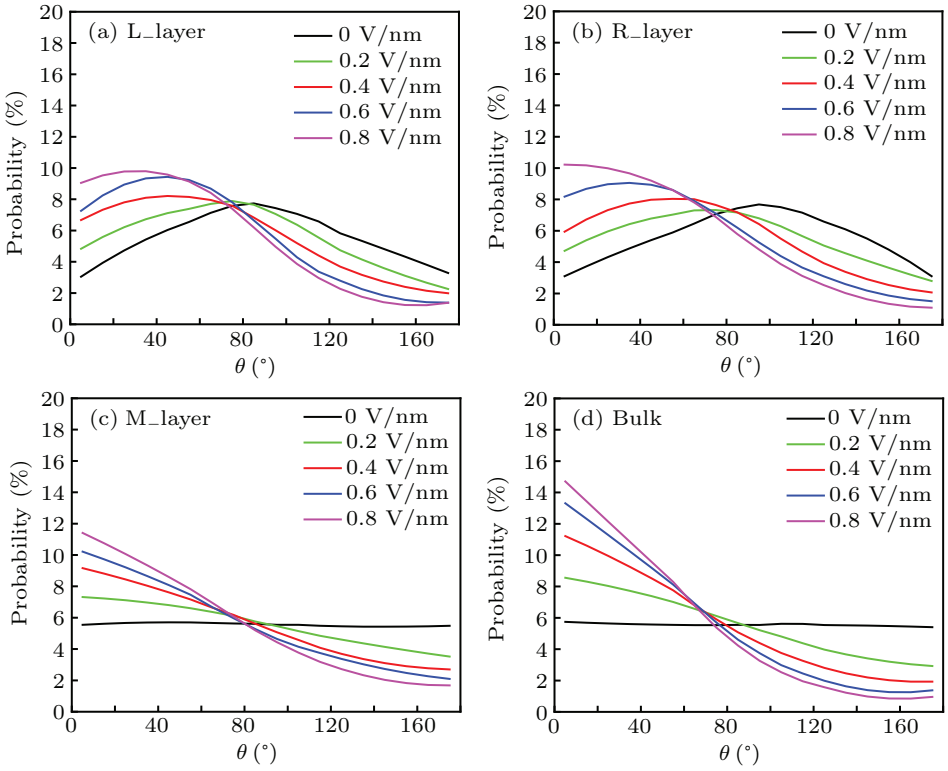


Fig. 4. Probability distribution for angle θ between water molecule dipole orientation and the z axis for a configuration when the plates are in contact $D = 1.9$ nm for different electric fields: (a) for the left interfacial layer ($0 \leq d \leq 0.6$ nm), (b) for the right interfacial layer (1.3 nm $< d \leq 1.9$ nm), (c) for the middle layer (0.6 nm $< d \leq 1.3$ nm), (d) for the bulk water.

The orientational structure of water molecules is sensitive to electric field. To observe how water molecules orient themselves adjacent to the plate as well as away from it under different electrical fields, we divided the inter-plate region of water into three different layers. Because N_2 molecules aggregate at the hydrophobic surface forming a non-uniform nitrogen layer (as shown in Figs. 3(a) and 3(b)), the interfacial water includes the water molecules adjacent to the hydrophobic plates (forming liquid-solid interface) and the water molecules near the nitrogen layer (forming water-nitrogen layer interface). Thus, the thickness of interfacial water layer is about 0.6 nm, approximately two layers of molecules. For simplicity, let d

be the perpendicular distance from the water molecule to the left plate. The left interfacial water layer contains the water molecules in the region of $\leq d \leq 0.6$ nm (denoted by L_layer). Similarly, the right interfacial water layer contains the water molecules in the region of 1.3 nm $< d \leq 1.9$ nm (denoted by R_layer). The region between them is considered as the middle layer with 0.6 nm $< d \leq 1.3$ nm (denoted by M_layer). The probability distributions of the orientational angle θ of the water molecule dipole to the z axis for the three water layers under different electric fields are shown in Fig. 4. Without an electric field, at the interface with the hydrophobic plates, the distributions of the dipole orientations for both the L_layer and R_layer (black lines shown in Figs. 4(a) and 4(b)) have a peak at around 85° and 95°, respectively. This indicates a preference for the dipole moment vector to avoid the surface normal, similar to the orientation of water molecules in the vicinity of hydrophobic surfaces found in the earlier studies.[40,41] In the M_layer, a flat distribution is observed (see Fig. 4(c)), which is the characteristic of a homogeneous fluid. It is similar to that of the bulk water outside the plates, as shown in Fig. 4(d). As the electric field increases, as is expected, the probability distribution profiles of the left and right interfacial layers shift obviously to the smaller orientational angle and the peak value increases correspondingly. Compared with the probability distribution curves of the M_layer and the bulk water (in Figs. 4(c) and 4(d)), the trend of water molecule orientation change is similar, the large-angle probability decreases, correspondingly, the small-angle probability increases. However, it should be noticed that the probability of small angle increases faster in the bulk water than in the M_layer, indicating that the interaction between the electric field and the bulk water is stronger than that between the electric field and the interplate water.

We further explored the mechanism of dewetting transition by examining the hydrogen bonds of water molecules inside of the plates. For comparison, we also calculated the hydrogen bonds of water molecules in bulk. The results are shown in Fig. 5. In the field-free case, for the bulk water, the average number of hydrogen bonds per water molecule is about 3.6. However, at the interface, the water molecules cannot maintain the same number of hydrogen bonds as they can be in the bulk. The average number of hydrogen bonds per water molecules decreases to 3.1. When a perpendicular electric field $E \leq 0.2$ V/nm is applied, the $\langle N_{\rm HB} \rangle$ for water molecules in both L_layer and M_layer remains nearly unchanged, except for a slight decrease in R_layer. It is indicated that the hydrogen bond network remains almost intact in this electric field range. Thus, in this range, the critical distance of dewetting transition is approximately unchanged (see Fig. 2(b)). As the electric field increases, the average number of hydrogen bonds for bulk water remains almost unchanged in the range $0 < E < 0.8$ V/nm. Surprisingly, the applied electric field breaks the symmetry of hydrogen bonds. The number of hydrogen bonds per water molecules in the L_layer is almost constant, while the number of hydrogen bonds in the R_layer decreases significantly with the increase of the electric field. It decreases from an initial value of 3.1 to 2.7 when E increases to 0.8 V/nm. The number of hydrogen bonds per water molecule in the middle water layer also decreases slightly.

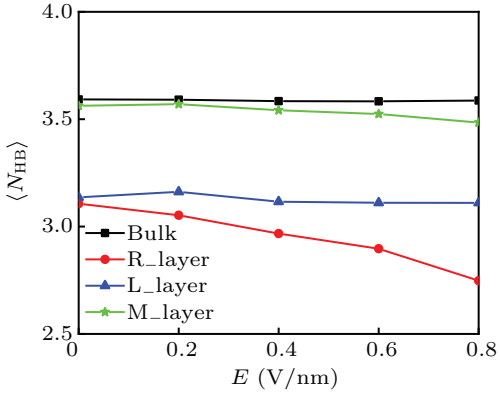


Fig. 5. Average number of hydrogen bonds per water molecule as a function of electric field for the configuration $D = 1.9$ nm. The interplate water molecules are divided into three layers: the left interfacial layer (L_layer), the right interfacial layer (R_layer) and the middle layer (M_layer), The corresponding regions are the same as those defined in Fig. 4.

Why are there more hydrogen bonds between water molecules at the right interfacial water layer broken by increasing the electric field than those at the left interfacial water layer and in the bulk water? This is resulted from the rearrangement of water molecules toward an external electric field. In the absence of external field, as shown in Figs. 4(a) and 4(b), the water molecules in the left water layer prefer to have a higher probability of facing the direction of the electric field ($\langle \theta \rangle = 84°$), while water molecules in the right water layer have a higher probability of facing the reverse direction of the electric field ($\langle \theta \rangle = 96°$). When an electric field is applied, the water molecules in the right water layer turn toward the electric field, that is, inward the hydrophobic surface. In the process, some hydrogen bonds are broken, resulting in a decrease in the number of hydrogen bonds. On the contrary, in the bulk, although the rotation of the water molecules increases with increasing the electric field, the water molecules can rotate and at the same time maintain a high degree of tetrahedral network connectivity. Thus, more hydrogen bonds are broken for the interfacial water as compared to the bulk water when the electric field increases. The fragility of the interfacial hydrogen bonds is the reason for the dewetting transition under the electric field.

We have also performed numerical simulations of the systems under a parallel electric field (along x axis). Our simulation results indicate that the effects of the parallel electric field

on the behavior of dewetting are very different from the perpendicular electric field. D_c decreases with the strength of a parallel electric field. Nitrogen molecules do not prefer to stay in the vicinity of the hydrophobic surfaces, dissolving in the bulk water. The main mechanism behind this phenomenon is the special structure of the hydrogen bonds network between water molecules adjacent to the hydrophobic surfaces, where dipoles of water molecules prefer to align parallel to the plates. When an external parallel electric field is introduced, the interaction between electric field and water molecules makes dipoles of water molecules align along the direction of the electric field. Thus, the ability of the perpendicular electric field to destroy the hydrogen bonding network between water molecules in the vicinity of plates is greater than the parallel electric field.

4. Conclusion

Our simulations and analyses reveal the effect of an external electric field on the dewetting behavior of a nanoscopic hydrophobic system. The perpendicular electric field applied to the hydrophobic plates can make the critical distance D_c for dewetting increase obviously. This indicates that the range of attractions between water-coated hydrophobic surfaces increases. The mechanism rests in aggregation of the nitrogen molecules governed by the external electric field. N_2 is in the formation of homo diatomic neutral molecule. The interaction between N_2 and the external electric field is zero. However, the hydrogen bonds between water molecules respond strongly to an electric field. The rearrangement of hydrogen bond network drives more nitrogen molecules to aggregate on the hydrophobic plates, resulting in the water molecules to be drained out of the nanoscale cavity between two hydrophobic plates.

It is found that the arrangement of water molecules confined between two nanoscale hydrophobic plates coated by nitrogen molecules is different from the bulk water. For the bulk water, it can adopt hydrogen-bonding patterns that keep the hydrogen bonds number constant. For the confined water, nanoscale confinement leads to ununiform distribution of dipole moment vector. The orientational preference for the dipole moment vector will be disrupted by the electric field. A fraction of hydrogen-bonding possibilities is thus lost near the right hydrophobic surface. As a result, water tends to move away from the interplate region. We also find that the effect of parallel electric filed is very different from the perpendicular electric filed. The parallel electric field can make the critical distance D_c for dewetting decrease dramatically. Our findings should be helpful for understanding the effects of the electric field on dewetting phenomena in biological systems.

Acknowledgement

Project supported by the National Natural Science Foundation of China (Grant No. 11875237).

References

[1] Chandler D 2005 *Nature* **437** 640
[2] Berne B J, Weeks J D and Zhou R 2009 *Annu. Rev. Phys. Chem.* **60** 85
[3] Blokzijl W and Engberts J B F N 1993 *Angew. Chem. Int. Ed. Engl.* **32** 1545
[4] Hummer G, Garde S, Garcia A E and Pratt L R 2000 *Chem. Phys.* **258** 349
[5] Ball P 2008 *Chem. Rev.* **108** 74
[6] Zhou R, Huang X, Margulis C J and Berne B J 2004 *Science* **305** 1605
[7] Liu P, Huang X, Zhou R and Berne B J 2005 *Nature* **437** 159
[8] Morrone J A, Li J and Berne B J 2012 *J. Phys. Chem. B* **116** 378
[9] Camilloni C, Bonetti D, Morrone A, Giri R, Dobson C M, Brunori M, Gianni S and Vendruscolo M 2016 *Sci. Rep.* **6** 28285
[10] Wolde P R t and Chandler D 2002 *Proc. Natl. Acad. USA* **99** 6539
[11] Hua L, Huang X, Liu P, Zhou R and Berne B J 2007 *J. Phys. Chem. B* **111** 9069
[12] Lum K, Chandler D and Weeks J D 1999 *J. Phys. Chem. B* **103** 4570
[13] Huang D M and Chandler D 2000 *Proc. Natl. Acad. Sci. USA* **97** 8324
[14] Huang X, Zhou R and Berne B J 2005 *J. Phys. Chem. B* **109** 3546
[15] Choudhury N and Pettitt B M 2007 *J. Am. Chem. Soc.* **129** 4847
[16] Rego N B, Xi E and Patel A J 2019 *J. Am. Chem. Soc.* **141** 2080
[17] Ishida N, Inoue T, Miyahara M and Higashitani K 2000 *Langmuir* **16** 6377
[18] Lou S T, Ouyang Z Q, Zhang Y, Li X J, Hu J, Li M Q and Yang F J 2000 *J. Vacuum Sci. Technol. B* **18** 2573
[19] Karpitschka S, Dietrich E, Seddon J R T, Zandvliet H J W, Lohse D and Riegler H 2012 *Phys. Rev. Lett.* **109** 066102
[20] Koishi T, Yoo S, Yasuoka K, Zeng X C, Narumi T, Susukita R, Kawai A, Furusawa H, Suenaga A, Okimoto N, Futatsugi N and Ebisuzaki T 2004 *Phys. Rev. Lett.* **93** 185701
[21] Agrawal A, Park J, Ryu D Y, Hammond P T, Russell T P and McKinley G H 2005 *Nano Lett.* **5** 1751
[22] Zhang X H, Zhang X, Sun J, Zhang Z, Li G, Fang H, Xiao X, Zeng X and Hu J 2007 *Langmuir* **23** 1778
[23] Li W, Zuo X, Zhou X and Lu H 2019 *J. Chem. Phys.* **150** 104702
[24] Zhang M, Zuo G, Chen J, Gao Y and Fang H 2013 *Sci. Rep.* **3** 1660
[25] Choudhury N and Pettitt B M 2005 *J. Am. Chem. Soc.* **127** 3556
[26] Li J, Liu T, Li X, Ye L, Chen H, Fang H, Wu Z and Zhou R 2005 *J. Phys. Chem. B* **109** 13639
[27] Zangi R and Berne B J 2008 *J. Phys. Chem. B* **112** 8634
[28] Zangi R 2011 *J. Phys. Chem. B* **115** 2303
[29] Remsing R C, Xi E, Vembanur S, Sharma S, Debenedetti P G, Garde S and Patel A J 2015 *Proc. Natl. Acad. Sci. USA* **112** 8181
[30] Wallqvist A and Berne B J 1995 *J. Phys. Chem.* **99** 2893
[31] Huang D M and Chandler D 2002 *J. Phys. Chem. B* **106** 2047
[32] Bolhuis P G and Chandler D 2000 *J. Chem. Phys.* **113** 8154
[33] Wolde P R T, Sun S X and Chandler D 2001 *Phys. Rev. E* **65** 011201
[34] Li J, Lu H and Zhou X 2020 *Nanoscale* **12** 12801
[35] Berendsen H J C, Postma J P M, Gunsteren W F V, DiNola A and Haak J R 1984 *J. Chem. Phys.* **81** 3684
[36] Berendsen H J C, Grigera J R and Straatsma T P 1987 *J. Phys. Chem.* **91** 6269
[37] Rappe A K, Casewit C J, Colwell K S, Goddard W A and Skiff W M 1992 *J. Am. Chem. Soc.* **114** 10024
[38] Darden T, York D and Pedersen L 1993 *J. Chem. Phys.* **98** 10089
[39] Wang C L, Li Z X, Li J Y, Xiu P, Hu J and Fang H P 2008 *Chin. Phys. B* **17** 2646
[40] Lee C Y, Mccammon J A and Rossky P J 1984 *J. Chem. Phys.* **80** 4448
[41] Sedlmeier F, Janecek J, Sendner C, Bocquet L, Netz R R and Horinek D 2008 *Biointerphases* **3** FC23